Program Digest, 2019 IEEE International Ultrasonics Symposium (IUS)
Glasgow, Scotland, October 6-9, 2019

Single-mode high frequency $LiNbO_3$ Film Bulk Acoustic Resonator

Marie Bousquet, Michaël Bertucchi, Pierre Perreau, Gaël Castellan, Catherine Maeder-Pachurka, Denis Mercier, Julien Delprato, Aurelio Borzi, Selsabil Sejil, Grégory Enyedi, Jérôme Dechamp, Marc Zussy, Pauline Sylvia Pokam Kuisseu, Frédéric Mazen, Christophe Billard, and Alexandre Reinhardt

Univ. Grenoble Alpes, CEA, LETI
Grenoble, France
marie.bousquet@cea.fr
christophe.billard@cea.fr
alexandre.reinhardt@cea.fr

***Abstract* — In this paper, Y+163°-cut $LiNbO_3$ (LNO) Film Bulk Acoustic Resonators (FBAR) with patterned bottom electrodes (AlSi or W) and a sacrificial layer cavity have been fabricated using a layer transfer process (4-inch). Unlike previous work based on films oriented towards the X axis [1], the Y+163° orientation provides a single resonance at 2.2 GHz, with an effective electromechanical coupling factor (k_t^2) of 26 %. Thanks to this single mode behavior and to the energy trapping induced by the heavy tungsten electrodes, the quality factor at antiresonance (Q_a) is increased to 600. Moreover a Temperature Coefficient of Frequency (TCF) of –45 ppm/°C is obtained. This demonstrates a significant improvement towards introducing $LiNbO_3$ as an alternative to AlN in Bulk Acoustic Wave (BAW) filters for the new generation of RF filters.**

Keywords — Lithium niobate ($LiNbO_3$), Film Bulk Acoustic Resonator (FBAR), film transfer, 5G

I. Introduction

As the number of frequency bands is expected to grow significantly with the deployment of the 5th Generation of mobile applications (5G), next generation of mobile communication systems require RF filters with increasingly stringent performances in terms of frequency, fractional bandwidth (FBW), temperature coefficient of frequency (TCF), steep skirts, insertion loss (IL) and compactness [2]. This opens the search for alternative piezoelectric materials with superior piezoelectric properties than those of conventional aluminum nitride (AlN, $k_t^2 = 6.5$ %) and its derivatives (e.g. $Al_{1-x}Sc_xN$, $k_t^2 = 9.2$ % [3]).

New solutions have recently come up, based on single crystal piezoelectric lithium tantalate ($LiTaO_3$) and lithium niobate ($LiNbO_3$) thin films: (i) Layered Surface Acoustic Waves (SAW) devices, also called I.H.P. (Incredible High Performance) [4], H.A.L. (Hetero Acoustic Layer structure) [5] or P.O.I. (Piezoelectric-On-Insulator) [6], based on a single crystal piezoelectric thin plate bonded on a substrate, (ii) Plate (Lamb) wave devices [7], also called Contour Mode Resonators (CMR) [8] or laterally excited bulk wave resonators (XBAR) [9], and (iii) Bulk Acoustic Waves (BAW) devices [1], [10].

A peculiarity of these technologies is that the electromechanical coupling coefficient can be adjusted by the choice of crystal orientation (from 5% up to 45% for bulk waves) [11]. Single-crystal lithium niobate $LiNbO_3$ (LNO) appears thus as an appealing candidate to replace AlN in BAW resonators [10]. Nevertheless, few reports dealt with single crystal LNO BAW resonators. Given that this material is difficult to grow as a single crystal thin film by conventional deposition techniques and displays piezoelectric properties inferior to its bulk counterpart [12], [13], film transfer approaches such as wafer bonding and mechanical thinning [10], [14], [15] or more recently crystal ion slicing (CIS) [1] are privileged (Table 1). Various crystal orientations (cuts) have been used: Y+36° [14], X [1], [10], [15], Y+45° [11]. Although high electromechanical coupling factors (53% [10] and 39% [1], respectively) were obtained, quality factors remain limited due to spurious resonances related to the existence of a second piezoelectrically active wave in X-cut LNO. On the contrary, the Y+163°-cut is known to support only one piezoelectrically coupled shear wave and is expected to provide less spurious resonances. With this orientation one can expect an

TABLE I. State of the art for $LiNbO_3$ (LNO) Film Bulk Acoustic Resonator (FBAR)

Ref	LNO cut (thickness)	f_r (GHz)	f_a (GHz)	Q	k^2 (%)
[14]	Y+36°-cut (25 µm)	0.50	NA	6770	5
[15]	X-cut (6.6 µm)	0.25	0.35	64	43
[10]	X-cut (20 µm)	0.10	0.12	210	53
[11]	Y+45°-cut (1 µm)	2.12	2.28	NA	NA
[1]	X-cut (0.6 µm)	2.42	2.99	250	39.2
[13]	Z-cut (0.41 µm)	2.90	2.97	73	5.8
Current work	Y+163°-cut (0.87 µm)	1.90	2.32	400	37.7
	Y+163°-cut (0.6 µm)	2.50	2.90	350	29.4
	Y+163°-cut (0.57 µm)	1.94	2.2	610	26

electromechanical coupling coefficient around 36.7 %. This crystal orientation has so far not been investigated for thin film bulk acoustic resonators.

In the present work, sub-micron thick single crystal Film Bulk Acoustic Resonators (FBAR) based on Y+163°-cut LNO with patterned bottom electrodes (AlSi and W) and a sacrificial layer cavity have been fabricated using a layer transfer process (4-inch). Then, we discuss electrical characterizations of the resonators, with a special emphasis on the electromechanical coupling and quality factor.

II. METHOD/RESULTS

A. *Resonators fabrication*

Three LNO Y+163°-cut FBAR devices were fabricated. They differ by their film transfer method (mechanical polishing, crystal ion slicing) and nature of the bottom electrode (AlSi, W). Fabrication details can be found in [1]. The electric response was measured using on-wafer probing and a Vector Network Analyzer.

B. *FBAR #1: LNO Y+163°-cut film obtained by mechanical polishing, with AlSi electrodes*

Fig.1 presents an optical micrograph of the fabricated device. The LNO film thickness is around 870 nm, while AlSi electrodes are 100 nm-thick. A typical admittance curve is shown in Fig. 2, and reveals a strong and clean resonance, with resonance and antiresonance frequencies of respectively 1.90 and 2.32 GHz, leading to a large electromechanical coupling factor of 37.7 %. As expected, only one wave is excited and, unlike previous works on LNO X-cut FBAR, there is no strong parasitic between resonance and antiresonance [1]. Quality factors at resonance and antiresonance are respectively 70 and 400, the quality factor at resonance being limited by the 0.8 Ω series resistance. The impedance ratio (Z_{max}/Z_{min}) is about 64 dB.

A comparison of the electric response with Mason's model (Fig. 2, blue curve) provides an excellent agreement with the electric response, revealing an intrinsic coupling coefficient (k_{int} = 36.7%) for the film in line with theoretical expectations for the bulk material. Nevertheless, an adjustment of propagation losses to fit the resonator quality factor leads to an intrinsic quality factor (*i.e.* free of the contribution of electrical losses) of 320. Although for LNO films obtained by mechanical polishing [10], [15] piezoelectric properties are almost fully preserved, the limitations in Q-factor are supposed to originate from high losses in the AlSi electrodes [16] and from thickness inhomogeneity of the piezoelectric film [15].

C. *FBAR #2: LNO Y+163°-cut film obtained by Crystal Ion Slicing (CIS), with AlSi electrodes*

In order to assess if the intrinsic quality factor is limited by thickness homogeneity, LNO FBAR with AlSi bottom electrodes were also prepared by Crystal Ion Slicing. Here the resonator stack is as follows: Al 100 nm / LNO Y+163°-cut 600 nm / AlSi 100 nm.

Fig. 3 shows the electric response of this device #2. The resonance and antiresonance frequencies are equal to 2.5 and

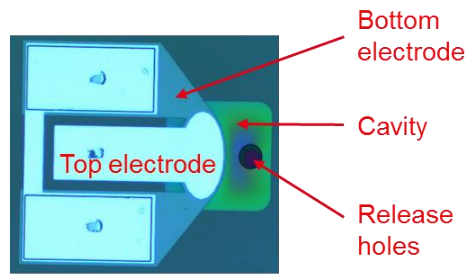

Fig. 1. Optical microscope photograph of a fabricated lithium niobate resonator with AlSi bottom electrodes by mechanical polishing (Device #1).

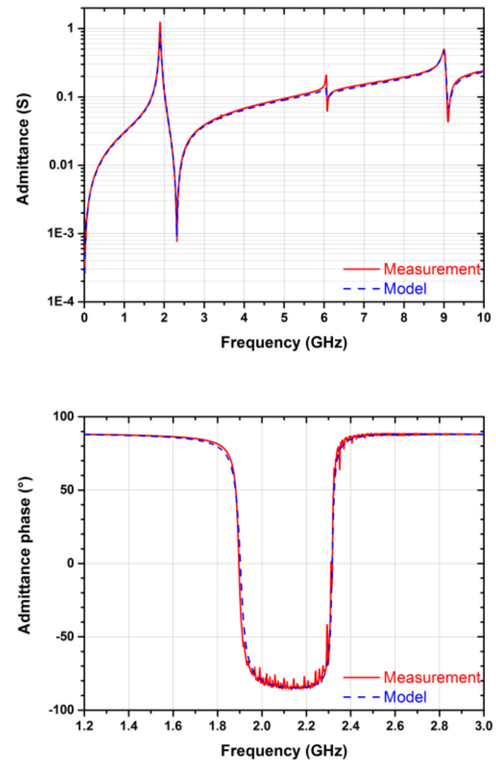

Fig. 2. Typical response of a Y+163°-cut $LiNbO_3$ FBAR with AlSi bottom electrodes obtained by mechanical polishing (Device #1) (continuous red curve) and fit of the electric response (Mason's model, dashed blue curve).

2.9 GHz. The ratio between maximum and minimum impedances is about 56 dB. A large electromechanical coupling factor of 29.4 % and a quality factor of 170 and 350 at resonance and antiresonance are obtained, with again the quality factor at resonance being limited by the series resistance. In comparison with device #1, the change in quality factor is marginal. So the limitation in quality factor seems rather to be attributed to losses in the AlSi electrodes.

Additionally, calculation of the Bode quality factor (Fig. 4) reveals a strong excitation of spurious modes located above the antiresonance frequency, at 3.3 GHz, but over a fairly large frequency range. It is already noticeable starting from 2.7 GHz, hence affecting the antiresonance. The frequency of 3.3 GHz

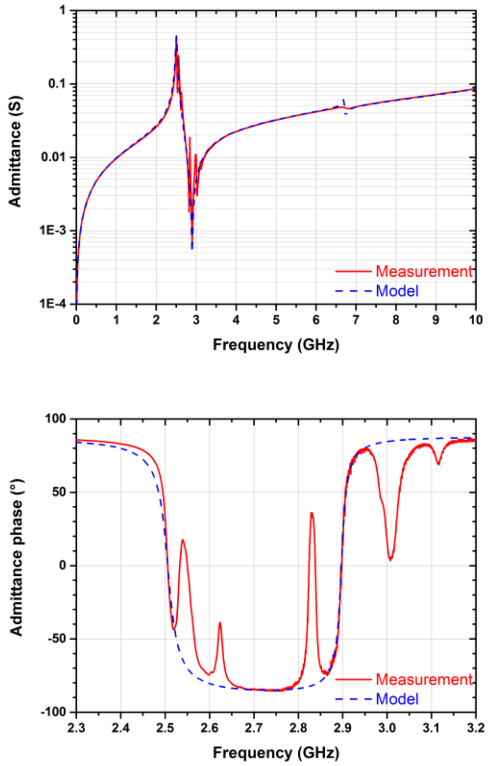

Fig. 3. Typical response of a Y+163°-cut $LiNbO_3$ FBAR with AlSi bottom electrodes obtained by Crystal Ion Slicing (Device #2).

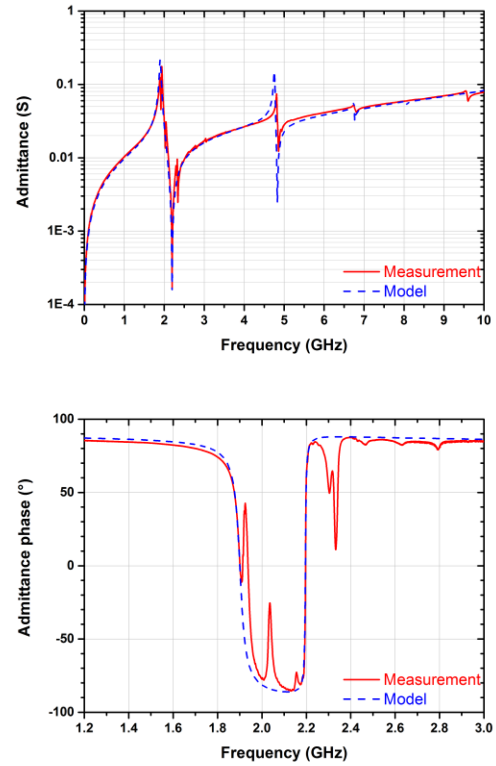

Fig. 5. Typical response of a Y+163°-cut $LiNbO_3$ FBAR with W bottom electrodes obtained by Crystal Ion Slicing (Device #3).

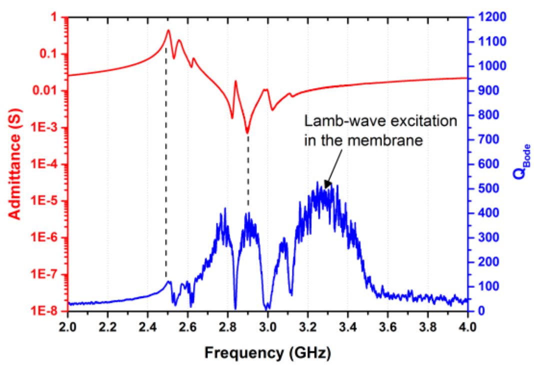

Fig. 4. Comparison of measured admittance and calculated Bode quality factor (Device #2).

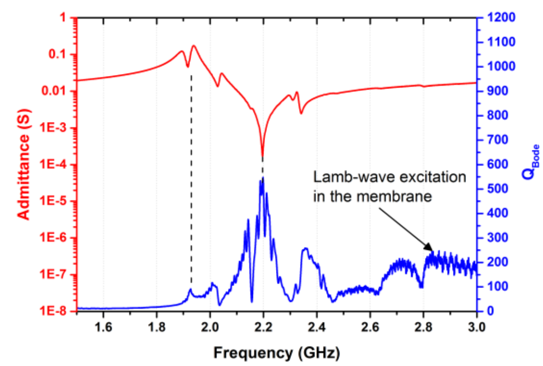

Fig. 6. Comparison of measured admittance and calculated Bode quality factor (Device #3).

corresponds to the cutoff frequency of the shear wave in the membrane when no metal mass loading occurs. Therefore, losses limiting the quality factor at antiresonance are mainly attributed to acoustic leakage in the membrane region surrounding the resonator and in the excitation of Lamb waves in this membrane despite the energy trapping condition being met over the whole resonance-antiresonance range. This is confirmed by the strong spurious resonances which are clearly visible in Fig. 4 and which are due to laterally propagating modes inside the resonator. A better energy trapping is therefore mandatory.

D. FBAR #3: LNO Y+163°-cut film obtained by Crystal Ion Slicing, with W bottom electrodes

For a better energy confinement, the bottom electrode was switched from AlSi to W. The material stack composing the resonator is composed as follows: Al 100 nm / LNO Y+163°-cut 570 nm / W 100 nm / SiO_2 100 nm, the additional SiO_2 coating protecting the W electrodes during membrane release by XeF_2 etching of the sacrificial layer. The LNO film was, as in the previous case, obtained by Crystal Ion Slicing. From the spacing between resonance (f_r = 1.94 GHz) and antiresonance (f_a = 2.20 GHz) frequencies, the electromechanical coupling factor is evaluated to 26 %. The quality factors are this time

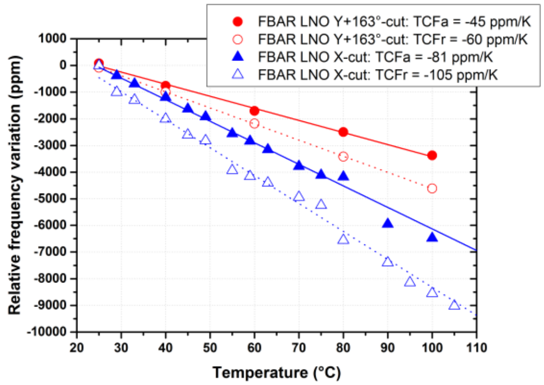

Fig. 7. TCF measurements of the 2.2 GHz Y+163°-cut $LiNbO_3$ FBAR device, with W patterned bottom electrode (Device #3). Red lines are the TCF measurements of the parallel peak and series peak; blue lines show the TCF of an X-cut $LiNbO_3$ resonator obtained in [1] for comparison.

evaluated to be 110 at resonance and 610 at antiresonance, pushing the impedance ratio to be around 60 dB (Fig. 5).

The introduction of W bottom electrodes seems particularly efficient, as Mason's model now requires an intrinsic quality factor of 800 to fit the electric response. The intrinsic coupling coefficient is fitted to 29.3%. The discrepancy reduction in the electromechanical coupling factor is attributed to the contribution of an un-compensated pad capacitance and possible post-transfer material defects which are still under investigation. Plotting the Bode quality factor versus frequency (Fig. 6) clearly shows that while Lamb waves continue to be excited above 3 GHz, the increased mass loading of W electrodes has shifted the whole electric response of the resonator away from this frequency region, hence reducing the leakage of acoustic power from the resonator into the surrounding membrane.

Finally, the temperature dependence of device #3 was investigated in the 25°C to 100°C range (Fig. 7). The TCFs of the series and the parallel resonances are equal to -61 ppm/K and -45 ppm/K, respectively, which is lower than the -80 ppm/K of X-cut $LiNbO_3$ FBARs [1].

III. Conclusions and Prospects

Y+163°-cut $LiNbO_3$ based FBARs were fabricated using film transfer approaches (mechanical polishing and crystal ion slicing) while including patterned bottom electrodes and a sacrificial layer cavity. We therefore managed to demonstrate resonators in the 2-3 GHz range, with electromechanical coupling factors in excess of 25% and a cleaner electric response than in previous works due to the suppression of the parasitic slow shear wave. Thanks to this single mode behavior and to the energy trapping induced by heavy tungsten electrodes, the quality factor at antiresonance (Q_a) was pushed towards 600. Future work will be devoted to further improve performances, in terms of quality factor, spurious resonances mitigation and temperature compensation.

Acknowledgments

This research was funded in part by Intel Corporation. This work has been performed with the help of the "Plateforme Technologique Amont" de Grenoble, with the financial support of the "Nanosciences aux limites de la Nanoélectronique" Fundation" and CNRS Renatech network.

References

[1] M. Gorisse, L. Dours, P. Perreau, A. Ravix, R. Lefebvre, G. Castellan, C. Maeder-Pachurka, M. Bousquet, A. Reinhardt, R. Bauder, H.-J. Timme, and H.-P. Friedrich, "High Frequency $LiNbO_3$ Bulk Wave Resonator", in Proc. IEEE International Frequency Control Symposium & European Frequency Time Forum (2019).

[2] A. Hagelauer, G. Fattinger, C. W. Ruppel, M. Ueda, K.-Y. Hashimoto, and A. Tag, "Microwave Acoustic Wave Devices: Recent Advances on Architectures, Modeling, Materials, and Packaging", IEEE Trans. Microwave Theory and Techniques 66, 4548 (2018).

[3] M. Akiyama, T. Kamohara, K. Kano, A. Teshigahara, Y. Takeuchi, and N. Kawahara, "Enhancement of piezoelectric response in scandium aluminum nitride alloy thin films prepared by dual reactive cosputtering", Adv. Mater. 2, 593 (2009).

[4] T. Takai, H. Iwamoto, Y. Takamine, H. Yamazaki, T. Fuyutsume, H. Kyoya, T. Nakao, H. Kando, M. Hiramoto, T. Toi, M. Koshino and N. Nakajima, "Incredible High Performance SAW resonator on Novel Multi-layerd Substrate", in Proc. IEEE International Ultrasonics Symposium, art. no. 7728455 (2016).

[5] M. Kadota and S. Tanaka, "Wideband acoustic wave resonators composed of hetero acoustic layer structure", Jpn J. Appl. Phys. 57, 07LD12 (2018).

[6] S. Ballandras, I. Radu, E. Courjon, I. Huyet, T. Baron, T. Laroche, A. Drouin, and F. Bernard, "New Generation of SAW Devices on Advanced Engineered Substrates Combining Piezoelectric Single Crystals and Silicon", in Proc. IEEE International Frequency Control Symposium & European Frequency Time Forum (2019).

[7] S. Gong and G. Piazza, "Design and Analysis of Lithium–Niobate-Based High Electromechanical Coupling RF-MEMS Resonators for Wideband Filtering", IEEE Trans. Microwave Theory and Techniques 61, 403 (2013).

[8] R. Wang, S. A. Bhave, and K. Bhattacharjee, "Low TCF Lithium Tantalate Contour Mode Resonators", in Proc. International Frequency Control Symposium, art. no. 6859998 (2014).

[9] V. Plessky, V. Plessky, S. Yandrapalli, P.J. Turner, L.G. Villanueva, J. Koskela and R.B. Hammond, "5 GHz laterally-excited bulk-wave resonators (XBARs) based on thin platelets of lithium niobate", Electron. Lett. 55, 98 (2019).

[10] A. Reinhardt, L. Benaissa, J.-B. David, N. Lamard, V. Kovacova, N. Boudou, E. Defaÿ, "Acoustic filters based on thin single crystal $LiNbO_3$ films: status and prospects", in Proc. International Ultrasonics Symposium, art. no. 6931726 (2014).

[11] Y. Osugi, T. Yoshino, K. Suzuki, and T. Hirai, "Single crystal FBAR with $LiNbO_3$ and $LiTaO_3$ piezoelectric substance layers", IEEE/MTT-S Int. Microwave Symposium, art. no. 4263960 (2007).

[12] A. Bartasyte, S. Margueron, T. Baron, St. Oliveri, and P. Boulet, "Toward High-Quality Epitaxial $LiNbO_3$ and $LiTaO_3$ Thin Films for Acoustic and Optical Applications", Adv. Mater. Interfaces 4, 1600998 (2017).

[13] M. Kadota, Y. Suzuki, and Y. Ito, "Properties of $LiNbO_3$ Thin Film Deposited by Chemical Vapor Deposition and Frequency Characteristics of Film Bulk Acoustic Wave Resonator", Jpn J. Appl. Phys. 50, 07HD10 (2011).

[14] D. Gachon, G. Lengaigne, S. Benchabane, H. Majjad, S. Ballandras, and V. Laude, "High Frequency Bulk Acoustic Wave Resonator Using Thinned Monocrystalline Lithium Niobate", in Proc. European Frequency Time Forum, art. no. 6230939 (2006).

[15] M. Pijolat, S. Loubriat, S. Queste, D. Mercier, A. Reinhardt, E. Defaÿ, C. Deguet, L. Clavelier, H. Moriceau, M. Aïd, and S. Ballandras, "Large electromechanical coupling factor film bulk acoustic resonator with X-cut $LiNbO_3$ layer transfer", Appl. Phys. Lett. 95, 182106 (2009).

[16] G. G. Fattinger, S. Marksteiner, J. Kaitila, and R. Aigner, "Optimization of Acoustic Dispersion for High Performance Thin Film BAW Resonators", in Proc. IEEE International Ultrasonics Symposium, art. no. 1603060 (2005).